Elemental Composition of the Soils using LIBS Laser Induced Breakdown Spectroscopy

Muhammad Aslam Khoso[1], Seher Saleem[1], Altaf H. Nizamani[1], Hussain Saleem[2], Abdul Majid Soomro[1], Waseem Ahmed Bhutto[1], Saifullah Jamali[1], Nek Muhammad Shaikh[1]

[1]Institute of Physics, University of Sindh, Jamshoro, Pakistan.
[2]Department of Computer Science, UBIT, University of Karachi, Karachi, Pakistan.

**Corresponding Author:*

Abstract
Laser induced breakdown spectroscopy (LIBS) technique has been used for the elemental composition of the soils. In this technique, a high energy laser pulse is focused on a sample to produce plasma. From the spectroscopic analysis of such plasma plume, we have determined the different elements present in the soil. This technique is effective and rapid for the qualitative and quantitative analysis of all type of samples. In this work a Q-switched Nd: YAG laser operating with its fundamental mode ($1064\ nm$ laser wavelength), 5 nanosecond pulse width, and 10 Hz repetition rate was focused on soil samples using $10\ cm$ quartz lens. The emission spectra of soil consist of Iron (Fe), Calcium (Ca), Titanium (Ti), Silicon (Si), Aluminum (Al), Magnesium (Mg), Manganese (Mn), Potassium (K), Nickel (Ni), Chromium (Cr), Copper (Cu), Mercury (Hg), Barium (Ba), Vanadium (V), Lead (Pb), Nitrogen (N), Scandium (Sc), Hydrogen (H), Strontium (Sr), and Lithium (Li) with different finger-prints of the transition lines. The maximum intensity of the transition lines was observed close to the surface of the sample and it was decreased along the axial direction of the plasma expansion due to the thermalization and the recombination process. We have also determined the plasma parameters such as electron temperature and the electron number density of the plasma using Boltzmann's plot method as well as the Stark broadening of the transition lines respectively. The electron temperature is estimated at $14611\ °K$, whereas the electron number density i.e. $4.1 \times 10^{16}\ cm^{-3}$ lies close to the surface.

Keywords:
Electron number density; Electron temperature; LIBS; Plasma plume; Spectroscopy;

1. Introduction

Laser-Induced Breakdown Spectroscopy (LIBS) is a fast and reliable analytical technique. In the past few years, significant advances have been made in the area of LIBS applications to the detection of the heavy and toxic elements present in the food, soil samples affecting humans and animal health. In this work, we have tried to provide comprehensive knowledge and data about the different percentages of the elements present in the soil of Sindh province in Pakistan. In this method, a high-intensity laser pulse from a Q- switched Nd: YAG laser is focused to target sample for the ablation of the sample in the form of the plasma plume [1][2][3].

In the literature, much of the experimental and the theoretical work is reported for this technique [7][8][11][32][38]. This technique (LIBS) exhibits very attractive features and become the most reliable, fast and eco-friendly in the field of materials analysis, process control, environmental monitoring, life sciences and has the capacity of multi-elemental detection, rapid response, very little or no sample preparation, high spectral resolution and high sensitivity [18][25][26][27][30]. Meanwhile, many experimental studies are reported in the literature about the characteristics of the soil plasma. Bublitz et. al. [16] presented the spectroscopic study of soil diagnostics. Sarah et. al. [40] has discussed the characteristics and forensic analysis of the soil sample. Hussain et. al. [43] measured the nutrients in greenhouse soils using Nd: YAG laser. Martin et. al. [36] determined the total carbon and nitrogen in the soil. Bustamante et. al. [24] used Laser induced breakdown spectroscopy for characterization of Ca in a soil depth profile. Xia-Fen Li et. al. [23] determined the temperature and electron number density of soil plasma generated by laser ablation fast pulse discharge plasma spectroscopy (LA-FPDPS) [39][45]. Ciucci et. al. [9] has developed the calibration-free laser-induced breakdown spectroscopy and argued that the plasma temperature and electron number density are the two main parameters for plasma characterization based on the measured plasma temperature and electron number density. Akhtar et. al. [22] has analyzed the elements of Pb and Cu in soil sample using laser-induced breakdown spectroscopy under an external magnetic field. Cao et. al. [10] used pulse laser ablation (PLA) to observe the big second-order non-linear optical response from sapphire substrates deposited ZnO thin films. Sheikh et. al. [34] studied spectroscopic studies of Zn plasma produced in the air through 1064, 532 and $355\ nm$ Q-switched Nd: YAG laser. Saji et. al. [20] studied optical emission spectroscopy of ZnO sample using $355\ nm$ laser from Nd: YAG laser [4][12][14][28][29][37]. In present work, Laser induced breakdown spectroscopic technique has been utilized for soil samples collected from the right bank of river Indus of Sindh province of Pakistan. From the spectroscopic analysis of the transition lines, we have found different toxic and nutritious elements present in the soil. We have also estimated the plasma parameters from the recorded emission spectrum.

Manuscript received June 5, 2024
Manuscript revised June 20, 2024
https://doi.org/10.22937/IJCSNS.2024.24.6.23

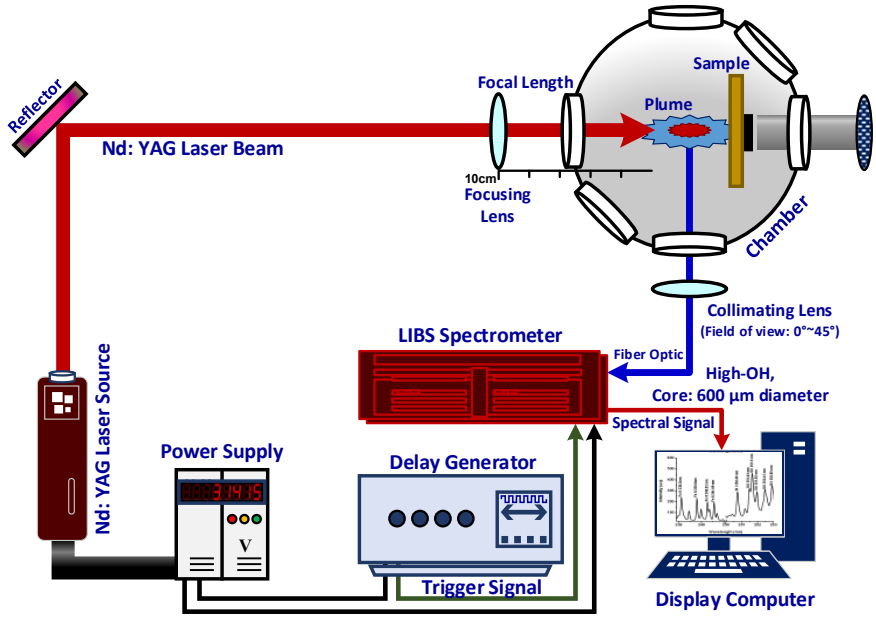

Fig.1. The experimental arrangement of LIBS (Laser Induced Breakdown Spectroscopy) method [20].

2. Sample Preparation

The soil samples were collected from the right bank of river Indus at the three and six inches depth from the wheat cropped field. The soil sample was dried at $100°C$ up to one hour in the microwave oven.

The samples were then grinded and powdered using Retsch Mortar Grinder RM-200. Then next it was filtered to obtain the required size using Sieving Machine Retsch AS-400. Than 10 $gram$ sample mix with 3 $gram$ wax using Swing mill HK-40.

Then 3 $gram$ of the whole mixed sample was wasted. The net 10 $grams$ were taken for the pallet preparation using Electro-hydraulic press PE-EL. The 10 $gram$ pallets of the sample were hence prepared for LIBS analysis.

3. Experimental Setup

The experimentation bench of Laser induced breakdown spectroscopy (LIBS) was set as shown in Fig.1. This experimental arrangement was adapted from Ref. [20]. For the ablation of the sample, we have used a high power Q-switched Nd: YAG laser pulse operating with 400 mJ at fundamental mode with a pulse duration of 5 ns and repetition rate of 10 Hz.

The laser energy was measured with the energy meter (Nova - Quantel, France). A reflecting glass is used for reflecting the laser beam and a focusing quartz lens of 10 cm focal lengths is used to focus the laser beam on the target material.

The estimated area of the laser spot on the target was approximately $\approx 3.0 \times 10^{-4}\ cm^2$. The target was mounted on the sample stage, which was rotated to provide a fresh surface after each laser pulse to avoid deep crater. The distance between the focusing lens and the sample was less than the focal length of the lens, this prevented any breakdown of the ambient gas (air) in front of the target.

The emission from the plasma plume was collected through an optical fiber (High-OH, Core diameter: 600 μm) with a collimating lens (0°~45° field of view) placed at a right angle to the laser producing plume. The LIBS2000 detection system is equipped with five spectrometers each having slit width of $5\mu m$, covering the range between 200 $nm \sim 700\ nm$.

Each spectrometer has a 2048 element linear CCD array and an optical resolution of $\approx 0.1\ nm$. The LIBS2000 detection system and the Q-switch of the Nd: YAG laser were synchronized. The LIBS2000 system triggered the Q-switch of the Nd: YAG laser and the flash lamp out of the Nd: YAG laser triggered the LIBS2000 detection system through a four-channel digital delay/Pulse generator (SRS DG 535).

The pulse energy of the Nd: YAG laser was varied through the OOI-LIBS software [13]. The output data were averaged for 10 laser shots. The data acquired simultaneously by all the five spectrometers were stored on a PC through the OOI-LIBS software for subsequent analysis.

Table-1. Trace elements found in Soil Sample with various wavelength(s) and concentrations.
These include Iron (***Fe***), Calcium (***Ca***), Titanium (***Ti***), Silicon (***Si***), Aluminum (***Al***), Magnesium (***Mg***), Manganese (***Mn***), Potassium (***K***), Nickel (***Ni***), Chromium (***Cr***), Copper (***Cu***), Mercury (***Hg***), Barium (***Ba***), Vanadium (***V***), Lead (***Pb***), Nitrogen (***N***), Scandium (***Sc***), Hydrogen (***H***), Strontium (***Sr***), and Lithium (***Li***).

Elements		1 Iron (*Fe*)					2 Calcium (*Ca*)				
Wavelength (*nm*)	1.	238.24	274.90	406.53	492.21	502.50	315.8	397.25	443.49	558.87	616.90
	2.	239.61	324.95	407.37	495.95	519.27	317.9	422.67	445.59	559.44	643.90
	3.	240.52	358.12	413.44	498.44	522.74	335.02	428.30	518.88	559.84	645.56
	4.	241.09	386.59	414.60	499.05	523.29	364.44	429.90	526.17	560.12	646.25
	5.	258.64	373.71	421.75	500.18	537.14	370.60	430.25	526.42	585.74	647.16
	6.	259.90	374.94	438.53	501.006	538.38	373.69	430.77	527.03	610.27	649.96
	7.	260.70	376.05	487.82	501.64	540.57	393.36	431.86	534.9	612.22	714.82
	8.	261.18	404.58	489.37	502.22	--	396.84	442.54	558.19	616.12	--

Elements		3 Titanium (*Ti*)		4 Silicon (*Si*)		5 Aluminum (*Al*)		6 Magnesium (*Mg*)		7 Manganese (*Mn*)	8 Potassium (*K*)
Wavelength (*nm*)	1.	323.45	334.27	250.49	252.82	256.79	364.92	279.01	285.21	274.02	344.05
	2.	323.71	336.24	251.43	252.85	257.50	358.70	279.55	516.73	274.73	372.13
	3.	324.05	337.35	251.61	263.12	308.21	394.40	279.77	517.26	403.28	399.18
	4.	326.26	338.46	251.92	288.15	309.27	396.15	280.27	518.36	407.99	400.12
	5.	332.46	521.03	252.41	319.22	--	--	--	--	--	532.36

Elements		9 Nickel (*Ni*)		10 Chromium (*Cr*)		11 Copper (*Cu*)		12 Mercury (*Hg*)		13 Barium (*Ba*)	
Wavelength (*nm*)	1.	357.18	361.93	425.43	428.93	324.75	327.30	398.39	614.10	553.32	440.68
	2.	361.04	490.44	427.48	--	325.22	--	542.52	--	493.40	--

Elements		14 Vanadium (*V*)		15 Lead (*Pb*)		16 Nitrogen (*N*)		17 Scandium (*Sc*)	18 Hydrogen (*H*)	19 Strontium (*Sr*)	20 Lithium (*Li*)
Wavelength (*nm*)	1.	275.63	277.85	363.95	261.43	588.99	589.59	316.09	656.42	421.42	--

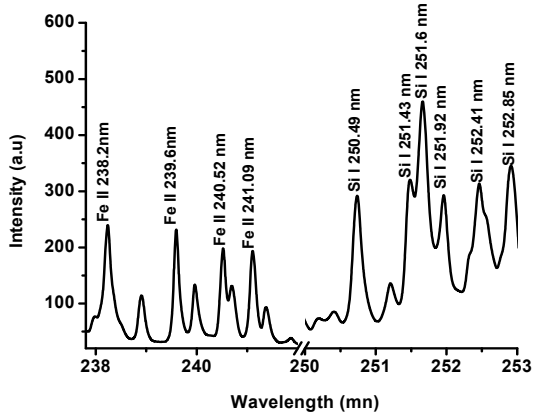

Fig.2 (a): Spectra in the range of 238 *nm* to 253 *nm* of Soil sample.

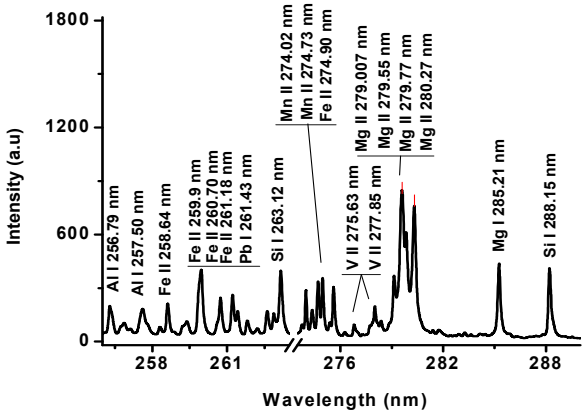

Fig.2 (b): Spectra in the range of 255 *nm* to 288 *nm* of Soil sample.

Table-2. Spectroscopic parameters used to calculate electron temperature.

Wavelength $\lambda\ (nm)$	Statistical Weight		Transition Probability $A_{ij}\ (s^{-1})$	Upper Level Energy $E_k\ (cm^{-1})$
	g_k	g_i		
335.02	3	5	8.90×10^7	45050.42
393.50	2	4	5.88×10^8	25414.40
534.94	5	5	1.08×10^8	362893.47
559.84	3	5	3.30×10^8	40719.84
616.12	5	5	1.60×10^7	36575.119

4. Results and Discussion

4.1 The Atomic Emission Spectrum of Soil Plasma

In the first set of experiment, we have focused on the elemental composition of the different elements present in the soil. For this purpose, we used the fundamental mode of a Q-switched Nd: YAG laser, having the laser irradiance of $4.5 \times 10^{10}\ W/cm^2$ was focused on the soil sample placed in air.

The emission spectrum from plasma plume was registered on the PC through OOI-LIBS software. The total range of the spectrum varies from $200{\sim}720\ nm$. The emission spectrum contains Iron (Fe), Calcium (Ca), Titanium (Ti), Silicon (Si), Aluminum (Al), Magnesium (Mg), Manganese (Mn), Potassium (K), Nickel (Ni), Chromium (Cr), Copper (Cu), Mercury (Hg), Barium (Ba), Vanadium (V), Lead (Pb), Nitrogen (N), Scandium (Sc), Hydrogen (H), Strontium (Sr), and Lithium (Li) as shown in Table-1.

A portion of the spectrum from $200{\sim}290\ nm$ is shown in Fig.2 (a) and Fig.2 (b). It was observed that the intensity of the Iron and Calcium is dominant as compared to the other elements (Vanadium, Scandium, Hydrogen, Lead, Nitrogen and Strontium) present in the soil.

The intensity of the transition line is associated with the population of such exciting level and it is also temperature-dependent of the plasma. The intensity variation of spectral lines is expressed by a relation via $Eq.(1)$ as given below [20][33][34][35].

$$I_{ij} = \frac{h\nu}{4\pi} N_i g_i A_{ij} \qquad \cdots (1)$$

In the above equation, I_{ij} shows the intensity, N_i shows the number density, g_i denotes statistical weight, A_{ij} shows the transition probability and i and j shows the lower level and upper level respectively.

To study the hydrodynamic nature of the plasma plume expansion, we have recorded the spectrums at different positions along the axial direction of the plasma. The spatial variation of few of the transition lines of Ca-II 393.36 nm, Ca-I 534.94 nm and Ca-I 559.74 nm are shown in Fig.3.

It is shown that close to the surface of the sample at around $0\ mm$, the intensity of the transition lines are strongest while becoming weakest at a distance of $2\ mm$ from the surface of the sample. This variation has indicated the thermalization and the recombination process of the plasma during its expansion along the axial direction.

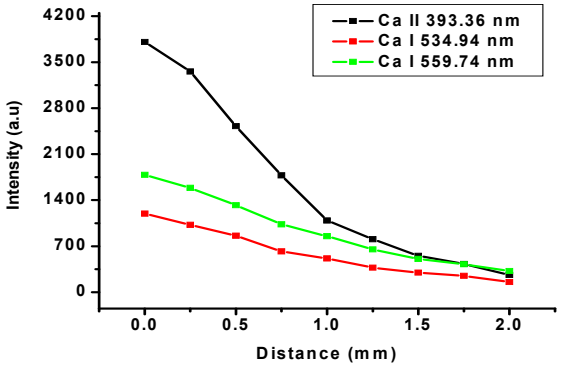

Fig.3. Spatial variation in the signal intensities of Ca-II 393.36 nm, Ca-I 534.94 nm and Ca-I 559.74 nm lines as function of distance $(0{\sim}2\ mm)$ from soil target surface.

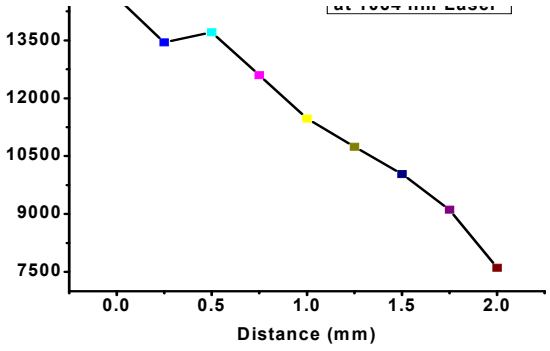

Fig.4. Electron temperature variation of soil plasma along with axial distance $(0{\sim}2\ mm)$.

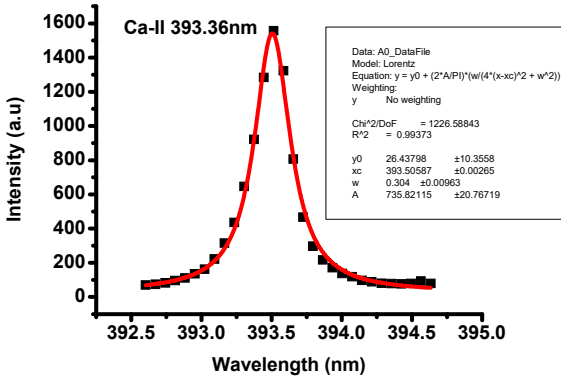

Fig.5. Optical transition line of Ca-II 393.36 nm the solid line represents the Lorentzian fit whereas dots show actual data.

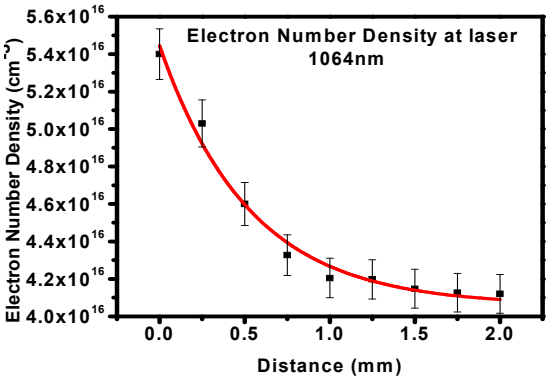

Fig.6. Electron number density variation of soil plasma along with axial distance (0~2 mm).

4.2 The Electron Temperature

Electron temperature is one of the very important parameters for the laser-produced plasma. In this work, the Boltzmann plot method is used to determine the electron temperature from the selected Calcium neutral transition lines. Boltzmann plot method adapted from [31] is given below by $Eq.(2)$.

$$ln\left(\frac{\lambda_{ki}I_{ki}}{A_{ki}g_k}\right) = ln\left(\frac{N}{Z}\right) - \left(\frac{E_k}{KT_e}\right) \qquad \cdots (2)$$

Where, λ_{ki} is the wavelength of the emission transition line, I_{ki} is the intensity of the emission transition line, A_{ki} is the transition probability, g_k is the statistical weight of the upper level, N is the upper-level population, Z is the partition function, E_k is the excitation energy, K is the Boltzmann constant and T_e is the electron temperature. To calculate electron temperature T_e selected neutral Calcium lines 335.02 nm, 534.94 nm, 585.74 nm and 616.12 nm respectively, the details of these transition lines are given in Table-2.

A plot of $ln\left({}^{\lambda_{ki}I_{ki}}/_{A_{ki}g_k}\right)$ versus upper-level energy yield a straight line having the slope ${}^{-1}/_{KT_e}$. The electron temperature is estimated from the slope. In the present experiment electron temperature T_e is estimated as 14611 $°K$ close to the plasma plume (0 mm) and 7607 $°K$ at (2 mm) away from plasma plume. The overall variation of electron temperature is a decreasing pattern as shown in Fig.4.

4.3 The Electron Number Density

The emission spectrum reveals noticeable line broadening due to the phenomenon of the "Doppler Effect" and "Stark Effect" etc. In the laser-produced plasma under the assumption of the local thermodynamic equilibrium (LTE), the Stark line broadening is the primary mechanism influencing these emission spectra [15][19][41][42].

The electron number density, related to the Full-Width Half Maximum (FWHM) of the Stark broadened lines is given by an expression [6][17].

$$\Delta\lambda_{1/2} = 2\omega\left(\frac{N_e}{10^{16}}\right) \qquad \cdots (3)$$

Whereas $\lambda_{1/2}$ is FWHM, ω is the impact parameter which can be determined from the literature [5][21][44], N_e is the electron number density.

To get the FWHM of the Stark broadened lines, we have fitted the Lorentzian fit on the singly ionized Calcium line at 393.36 nm is identified as follows and shown in Fig.5.

$$3p^6\ 4s\ {}^2p_{3/2} \rightarrow 3p^5\ 4s\ {}^2S_{1/2}$$

The calculated value of the electron number density close to the surface approximately at 0 mm distance is about $5.5 \times 10^{16}\ cm^{-3}$ and it decreases up to $4.1 \times 10^{16}\ cm^{-3}$ at 2 mm distance along the axial direction. The decreasing variation of electron number density is due to multiple reasons such as the recombination of plasma etc. The variation of electron number density along with distance is shown in Fig.6.

5. Conclusion

We have studied the elemental characterization of the laser-produced plasma of the soil samples taken from nearby to the Indus River Sindh Pakistan. We have determined Iron (Fe), Calcium (Ca), Titanium (Ti), Silicon (Si), Aluminum (Al), Magnesium (Mg), Manganese (Mn), Potassium (K), Nickel (Ni), Chromium (Cr), Copper (Cu), Mercury (Hg), Barium (Ba), Vanadium (V), Lead (Pb), Nitrogen (N), Scandium (Sc), Hydrogen (H), Strontium (Sr), and Lithium (Li) elements present in the soil. The concentration of the Iron and Calcium is maximum as compared to the other elements.

We have also observed some heavy elements in the soil. The intensity of transition lines is higher close to the target surface and becomes weaker as the detector moves away from the target surface.

Meanwhile, we have also determined the plasma parameters such as electron temperature and the electron number density using the Boltzmann plot method and the Stark broadening of the transition lines respectively. The electron temperature varies from $14611°K$ to $7607°K$ at a different axial distance from $0\ mm$ to $2\ mm$ from target sample, whereas the electron number density varies from $5.5 \times 10^{16}\ cm^{-3}$ to $4.1 \times 10^{16}\ cm^{-3}$ at the distance of about range $0\ mm$ to $2\ mm$ away from the target surface.

The maximum value of electron number density is close to the target surface at $0\ mm$ and follows decreasing when plasma getting expansion from away the target surface. The intensity, as well as the shift in transition lines decreases due to plasma recombination.

References

[1] A. H. Nizamani, B. Rasool, M. Tahir, N. M. Shaikh, H. Saleem, (2013), "Adiabatic ION Shuttling Protocols in Outer-Segmented-Electrode Surface ION Traps," International Journal of Scientific & Engineering Research (IJSER), 4(6), 3055-3061.

[2] A. H. Nizamani, M. A. Rind, N. M. Shaikh, A. H. Moghal, H. Saleem, (2013), "Versatile Ultra High Vacuum System for ION Trap Experiments: Design and Implementation," Intl. Journal of Advancements in Research & Technology, USA, 2(5).

[3] A. H. Nizamani, S. A. Buzdar, B. Rasool, N. M. Shaikh, H. Saleem, (2013), "Computer-based Frequency Drift Control of Multiple LASERs in Real-Time," International Journal of Scientific & Engineering Research (IJSER), 4(6), 3038.

[4] A. M. Soomro, W. A. Bhutto, A. H. Nizamani, H. Saleem, M. Y. Soomro, M. A. Khaskheli, N. M. Shaikh, (2019), "Controllable Growth of Hexagonal BN Monolayer Sheets on Cu Foil by LPCVD," IJCSNS International Journal of Computer Science and Network Security, vol. 19, no. 6.

[5] A. Safi, B. Campanella, E. Grifoni, S. Legnaioli, G. Lorenzetti, S. Pagnotta, F. Poggialini, L. Ripoll-Seguer, M. Hidalgo, V. Palleschi, (2018), "Multivariate Calibration in Laser-Induced Breakdown Spectroscopy Quantitative Analysis: The Dangers of a 'Black Box' Approach and How to Avoid Them, Spectrochimica Acta Part B: Atomic Spectroscopy Volume 144, (46-54)

[6] D. A. Cremers and L. J. Radzimski, (2006), "Handbook of Laser-Induced Breakdown Spectroscopy", Wiley, Chichester.

[7] E. Tognoni, V. Palleschi, M. Corsi and G. Cristoforetti, (2002), "Quantitative Micro-Analysis by Laser-Induced Breakdown Spectroscopy: A Review of the Experimental Approaches," Spectrochimica Acta Part B: Atomic Spectroscopy 57(7), 1115-1130.

[8] G Cristoforetti, S Legnaioli, V Palleschi, A Salvetti, E Tognoni, P A Benedetti, F Brioschi, and F Ferrario, (2006), "Quantitative Analysis of Aluminium Alloys by Low-Energy, High-Repetition Rate Laser-Induced Breakdown Spectroscopy," Journal of Analytical Atomic Spectrometry 21, no. 7, 697-702.

[9] G. Murtaza, Nek M Shaikh, G. A. Kandhro, M. Ashraf, (2019), "Laser Induced Breakdown Optical Emission Spectroscopic Study of Silicon Plasma" Spectrochimica Acta Part A: Molecular and Biomolecular Spectroscopy, 223 (117374).

[10] H. Cao, J. Y. Wu, H. C. Ong, J. Y. Dai and R. P. H. Chang, (1998), "Second Harmonic Generation in Laser Ablated Zinc Oxide Thin Films", Appl Phys Lett 73(5):572–574.

[11] H. R. Griem, (1997), "Principles of Plasma Spectroscopy", Cambridge Univ. Press, Cambridge.

[12] H. Saleem & et al., (2012), "Review of Various Aspects of Radio Frequency IDentification (RFID) Technology," International Organization for Scientific Research - Journal of Computer Engineering (IOSR-JCE), vol. 8, no. 1.

[13] H. Saleem & et al., (2019), "Imposing Software Traceability and Configuration Management for Change Tolerance in Software Production," IJCSNS International Journal of Computer Science and Network Security, vol. 19, no. 1.

[14] H. Saleem, A. H. Nizamani, W. A. Bhutto, A. M. Soomro, M. Y. Soomro, A. Toufik, (2019), "Two Dimensional Natural Convection Heat Losses from Square Solar Cavity Receiver," IJCSNS International Journal of Computer Science and Network Security, vol. 19, no. 4.

[15] J. B. Simeonsson and A. W. Miziolek, (1994), "Spectroscopic Studies of Laser-Produced Plasma Formed in CO and CO_2 using 193, 266, 355, 532 and 1064 nm Laser Radiation," Appl. Phy. B 59, 1-9.

[16] J. Bublitz, C. Dolle, W. Schade, A. Hartmann and R. Horn, (2001), "Laser-Induced Breakdown Spectroscopy for Soil Diagnostics," European Journal of Soil Science 52, 305-312.

[17] J. C. G. Sande, C. N. Afonso, J. L. Escudero, R. Serna, F. Catalina, and E. Bernabeu, (1992), "Optical Properties of Laser-Deposited a-Ge Films: A Comparison with Sputtered and e-Beam-Deposited Films", J.Appl. Opt. 31, 6133-6138.

[18] J. Kaiser, M. Galiová, K. Novotny, L. Reale, K. Stejska, O. Samek, R. Malina, K. Páleníková, V. Adam and R. Kizek, (2007), "Utilization of the Laser Induced Plasma Spectroscopy for Monitoring of The Metal Accumulation in Plant Tissues with High Spatial Resolution", Mod. Res. Educat. Top. Microsc. 1, 434–441.

[19] J. P. Singh, and S. N. Thakur, (2007), "Laser-Induced Breakdown Spectroscopy", Elsevier, Amsterdam, Netherland.

[20] K. J. Saji, N. V. Joshy and M. K. Jayaraj, (2006), "Optical Emission Spectroscopic Studies on Laser Ablated Zinc Oxide Plasma," Jour. of Appl. Phys. 100:043302 (5).

[21] Konjević, N., Lesage, A., Fuhr, J. R., & Wiese, W. L., (2002), "Experimental Stark Widths and Shifts for Spectral Lines of Neutral and Ionized Atoms (A Critical Review of Selected Data for the Period 1989 through 2000)", Journal of Physical and Chemical Reference Data, 31(3), 819-927.

[22] M. Akhtar, A. Jabbar, N. Ahmed, S. Mahmood, Z. A. Umar, R. Ahmed and M. A. Baig, (2019), "Analysis of Lead and Copper in Soil Samples by Laser-Induced Breakdown Spectroscopy under External Magnetic Field", Applied Phy B. 25:110.

[23] M. Ashraf, Nek M Shaikh, G. A. Kandhro, G. Murtaza J. Iqbal, A. Iqbal, S. Ali Lashari, (2020), "Energy Penetrated and Inverse Bremsstrahlung Absorption Coefficient in Laser Ablated Germanium Plasma," Journal of Molecular Structure, 1203 (127412).

[24] M. F. Bustamante, C. A. Rinaldi and J. C. Ferrero, (2002), "Laser-Induced Breakdown Spectroscopy Characterization of Ca in Soil Depth Profile", Spectr Acta Part B 57, 303-309.

[25] M. Hassan, M. Abdel Hamied, A. H. Hanafy, R. Fantoni and M. A. Harith, (2011), "Laser Monitoring of Phyto Extraction Enhancement of Lead Contaminated Soil Adopting EDTA and EDDS", AIP Conf. Proc. 1380, 93–100.

[26] M. Hassan, M. Sighicelli, A. Lai, F. Colao, A. H. H. Ahmed, R. Fantoni and M. A. Harith, (2008), "Studying the Enhanced Phyto Remediation of Lead Contaminated Soils via Laser Induced Breakdown Spectroscopy", Spectr. Acta Part B 63, 1225–1229.

[27] M. S. Gomes, D. S. Junior, L. C. Nunes, G. G. A. Carvalho, F. O. Leme and F. J. Krug, (2011), "Evaluation of Grinding Methods for Pellets Preparation Aiming at the Analysis of Plant Materials by Laser Induced Breakdown Spectrometry", Talanta 85, 1744–1750.

[28] M. Y. Channa, A. H. Nizamani, A. M. Soomro, H. Saleem, W. A. Bhutto, M. Y. Soomro, M. A. Khaskheli, N. M. Shaikh, (2019), "Vertical Ion Shuttling Protocols for Multi-Strip Surface Ion Traps," IJCSNS International Journal of Computer Science and Network Security, vol. 19, no. 7.

[29] M. Y. Channa, A. H. Nizamani, H. Saleem, W. A. Bhutto, A. M. Soomro, and M. Y. Soomro, (2019), "Surface Ion Trap Designs for Vertical Ion Shuttling," IJCSNS International Journal of Computer Science and Network Security, vol. 19, no. 4.

[30] Mohammed A. Hameed, Ahmed S. A. Al-Ali, Omar A. Ali and Ndher I. Mohammed, (2019) "Determination of the Fertility of Southern Iraqi Soil using Laser-Induced Breakdown Spectroscopy System" Journal of Physics: Conf. Series 1279 (012060).

[31] N. Ahmed, R. Ahmed, M. Rafiqe and M. A. Baig, (2016), "A Comparative Study of Cu-Ni Alloy using LIBS, LA-TOF, EDX and XRF", Laser and Particle Beam, 16: 0263-0346.

[32] N. M. Shaikh, A. H. Nizamani, A. H. Moghal, M. A. Rind. (2013). "Spectroscopic Studies of Copper Plasma Produced by Laser Ablation", Sindh Univ. Jour. (Sci. Ser.) Vol.45 (2) Page 399-404.

[33] N. M. Shaikh, B. Rashid, S. Hafeez, Y. Jamil and M. A. Baig, (2006), "Measurement of Electron Density and Temperature of a Laser-Induced Zinc Plasma", Jour. of Phys., Applied Phys. 39 (7), 1384.

[34] N. M. Shaikh, S. Hafeez, B. Rashid and M. A. Baig, (2007), "Spectroscopic Studies of Laser Aluminum Plasma using Fundamental, Second and Third Harmonics of a Nd: YAG Laser", The Eur. Phys. Jour. 44 (2), 371-379.

[35] N. M. Shiakh, S. Hafeez and M. A. Baig, (2007)," Plasma Properties of Laser-Ablated Strontium Target", Jour. of Applied Phys. 103 (8), 083117.

[36] P. D. Martin, D. F. Malley, G. Manning and L. Fuller, (2002), "Determination of Soil Organic Carbon and Nitrogen at the Field Level using Near-Infrared Spectroscopy", Can. J. soil. sci. 82, 413-422.

[37] R. Chand, Saeeduddin, M. A. Khaskheli, A. M. Soomro, H. Saleem, W. A. Bhutto, A. H. Nizamani, M.Y. Soomro, N. M. Shaikh, S. V. Muniandy, (2019), "Fractal Analysis of Light Scattering Data from Gravity-Driven Granular Flows," IJCSNS International Journal of Computer Science and Network Security, vol. 19, no. 7.

[38] R. Noll, (2012), "Laser-Induced Breakdown Spectroscopy", In Laser-Induced Breakdown Spectroscopy, pp. 7-15. Springer-Verlag, Berlin Heidelberg.

[39] S. A. Buzdar, M. A. Khan, A. Nazir, M. A. Gadhi, A. H. Nizamani, H. Saleem, (2013), Effect of Change in Orientation of Enhanced Dynamic Wedges on Radiotherapy Treatment Dose. IJoART, 2, 496-500.

[40] S. C. Jantzi and J. R. Almirall, (2011), "Characterization and forensic analysis of soil samples using laser-induced breakdown spectroscopy (LIBS)", Anal Bioanal Chem 400, 3341–3351.

[41] S. Jamali, W. A. Bhutto, A. H. Nizamani, H. Saleem, M. A. Khaskheli, A. M. Soomro, A. G. Sahito, N. M. Shaikh and S. Saleem, (2019), "Spectroscopic Analysis of Lithium Fluoride (LiF) using Laser Ablation", IJCSNS, 19. 8: 127 – 134.

[42] S. Yamada, S. Oguri. A. Morimoto, T. Shimizu, T. Minamikawa, and Y. Yonezawa, (2000), "Preparation of Epitaxial Ge Film on Si by Pulsed Laser Ablation using Molten Droplets", Jpn. J. Appl. Phys. 39, 278.

[43] T. Hussain, M. A. Gondal, Z. H. Yamani and M. A. Baig, (2007), "Measurement of Nutrients in Green House Soil with Laser Induced Breakdown Spectroscopy", Environ Monit Assess 124, 131–139.

[44] V. K. Unnikrishan, K. Alti, V. B. KArtha, C. Santhosh, G. P. Gupta and B. M. Suri, (2010), "Measurements of Plasma Temperature and Electron Density in Laser-Induced Copper Plasma by Time-Resolved Spectroscopy of Neutral Atom and Ion Emissions", Pramana-J. Phys., 74, 6.

[45] W. A. Bhutto, A. M. Soomro, A. H. Nizamani, H. Saleem, M. A. Khaskheli, A. G. Sahito, R. Das, U. A. Khan, S. Saleem, (2019), "Controlled Growth of Zinc Oxide Nanowire Arrays by Chemical Vapor Deposition (CVD) Method," IJCSNS International Journal of Computer Science and Network Security, vol. 19, no. 8.